Contribution No. 5629 from the Arthur Amos Noyes Laboratory of Chemical Physics, California Institute of Technology, Pasadena, California 91125

Nucleophilic Reactions of Anions with PF_3 and OPF_3 in the Gas Phase by Ion Cyclotron Resonance Spectroscopy

S. A. SULLIVAN and J. L. BEAUCHAMP*

Received October 18, 1977

Ion cyclotron resonance techniques are employed in the examination of the gas-phase reactions of PF_3 and OPF_3 with anionic bases, including NH_2^-, OH^-, $CH_3CH_2O^-$, HNO^-, HS^-, SF_6^-, and SF_5^-. Evidence is presented which suggests that all reactions proceed by initial attack at phosphorus, with products resulting from decomposition of chemically activated intermediates. The energetics of intermediates inferred in these processes are related to the Lewis acidities of OPF_3 and PF_3. With fluoride ion as a reference base, OPF_3 is found to be more acidic than PF_3, with $D(OPF_3\text{-}F^-) = 58.9 \pm 0.4$ kcal/mol and $D(PF_3\text{-}F^-) = 50 \pm 5$ kcal/mol.

Introduction

Phosphorus, like other second-row elements, is capable of hypervalent bonding[1] as shown by the existence of pentavalent phosphoranes PR_5 and phosphoryl compounds OPR_3 in addition to the expected trivalent phosphines PR_3. Many studies of these compounds have focused on processes involving nucleophilic attack at phosphorus.[1,2a,b] Both P(III) and P(V) are susceptible to nucleophilic attack in solution. The reactions of tetracoordinate P(V) compounds, and phosphate esters in particular, have been examined more extensively because of their relationship to processes in biological systems.[3]

A somewhat complex situation is suggested by mechanistic studies of nucleophilic substitution at P(V). Isotopic exchange during hydrolysis of alkyl phosphoryl compounds by bases B^- implicates the formation of pentavalent P(V) anionic intermediates (I).[1,4] Similar experiments, with phosphorus bearing

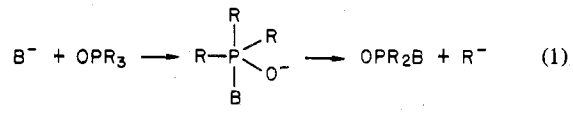

$$B^- + OPR_3 \longrightarrow R\text{-}P(R)(R)(O^-)(B) \longrightarrow OPR_2B + R^- \quad (1)$$

I

more electronegative substituents (e.g., R = CH_3O, Cl), are consistent with a direct displacement mechanism through a transition state like I.[1,5] The inference of reaction mechanisms in these systems is complicated[6] by the presence of two distinct ligand sites in the proposed intermediates. Analogous to PF_5,[7] the intermediates are expected to have trigonal-bipyramidal structures, with a preference for axial binding of electronegative substituents.[1] Structures and the mode of decomposition of reaction intermediates or transition states may thus be strongly moderated by the substituents on phosphorus.

The possibility of the formation of a hypervalent tetracoordinated phosphorus anion as an intermediate in nucleophilic substitution at phosphorus in tertiary phosphines (eq 2) has recently been considered by Kyba.[8] He observes that such processes occur with complete inversion at phosphorus and do not allow for pseudorotation in potential intermediates (e.g., II). For all intents and purposes nucleophilic substitution at P(III) is a classical S_N2 process with no formation of an intermediate.

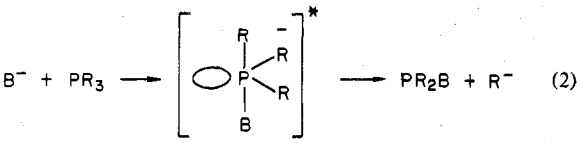

$$B^- + PR_3 \longrightarrow [R\text{-}P(R)(R)(B)]^* \longrightarrow PR_2B + R^- \quad (2)$$

II

Recent ion cyclotron resonance (ICR) studies have considered gas-phase reactions of anionic bases with fluorinated alkenes,[9] alkyl formates,[10] and other halogenated carbonyls.[11] Observed products are rationalized as the results of multiple-bond rearrangements and dissociation of chemically activated anionic intermediates.[9-12] Often it is possible to separately study the energetics of the reaction intermediates in these processes. For example, the tetrahedral adduct III is formed in eq 3 by chloride transfer.[12a]

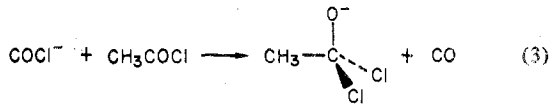

$$COCl^- + CH_3COCl \longrightarrow CH_3\text{-}C(O^-)(Cl)(Cl) + CO \quad (3)$$

III

In this laboratory we have extended our investigations of negative ion reaction mechanisms by examining the interaction of anions with phosphorus compounds. Preliminary studies of the reactions of strong bases with trimethyl phosphate[13] indicate that reaction 4 is the major process with CD_3O^-. The

$$CD_3O^- + OP(OCH_3)_3 \rightarrow O_2P(OCH_3)_2^- + CH_3OCD_3 \quad (4)$$

absence of deuterium incorporation into the ionic product in reaction 4 suggests that nucleophilic attack occurs at carbon rather than phosphorus. This somewhat surprising result is in contrast to solution reactions in which strong bases preferentially attack phosphorus.[14] Furthermore, by analogy with the gas-phase reactions of fluoroalkyl silanes (i.e., CH_3SiF_3) in mixtures with SF_6,[15] it was expected that F^--transfer adducts could also be formed with phosphate esters by transfer from F^- donors, for example, eq 5. Formation of such adducts may

$$SF_5^- + OP(OR)_3 \rightarrow OP(OR)_3F^- + SF_4 \quad (5)$$

be important as a method of soft ionization useful in chemical ionization mass spectrometry.[16] All attempts to form F^- adducts with phosphate and phosphite esters have failed.[13] This suggests that these compounds are very weak Lewis acids.

The above results provided the impetus for the present study in which we have examined the nucleophilic reactions of anionic bases, including NH_2^-, OH^-, $CH_3CH_2O^-$, HNO^-, and HS^-, with OPF_3 and PF_3. The electronegative fluorine ligands should decrease electron density at phosphorus, significantly enhancing its susceptibility to nucleophilic attack. Similarly, the stability of fluoride adducts OPF_4^- and PF_4^- should be considerably greater compared to adducts of phosphorus esters.

Experimental Section

Experiments were performed using an ICR spectrometer built in this laboratory, incorporating a 15-in. magnet capable of observing up to m/e 800. Instrumentation and experimental techniques of ICR spectroscopy have been described in detail previously.[17,18] Pressure was measured using a Schulz-Phelp ion gauge calibrated against a MKS Baratron Model 90-H1 capacitance manometer at higher pressures. Pressure measurements are the major source of error (±20%) in reaction rate constants.

Negative ion trapping techniques have been described elsewhere.[19] In a typical trapped ion experiment, the precursor to the reagent base was admitted to the analyzer, followed by addition of one or two other compounds to be investigated. Independent pressure control allows for variation of the partial pressures of each component. Total

0020-1669/78/1317-1589$01.00/0 © 1978 American Chemical Society

pressures normally were below 5×10^{-6} Torr, to minimize ion loss. Reaction rate constants are determined from limiting slopes for the disappearance of reactant ions in semilog plots of the variation of ion abundance with time.

Reactivity of ions in mixtures of neutrals may also be examined by observation of the variation of single-resonance ion intensities as a function of component partial pressure. Analytical methods for the calculation of reaction rates using ICR pressure studies have been described.[20]

The major ions produced by thermalized electron attachment in SF_6 are SF_6^- (95%) and SF_5^- (5%). Both ions are unreactive toward SF_6.[21] In a similar manner, the alkoxide ion $C_2H_5O^-$ is produced in CH_3CH_2ONO.[22] Primary ions CH_2CHO^- (17%) and HNO^- (10%) are also formed by electron attachment. The only reaction product ion detected is NO_2^-, which is formed on reaction of $CH_3CH_2O^-$ with the precursor nitrite. This reaction is minimized by maintaining low partial pressure of nitrites.

Reagent negative ions NH_2^-, HO^-, and HS^- are formed in NH_3, H_2O, and H_2S, respectively.[23,24] Resonance electron capture processes (4.0–8.0 eV) initiate NH_2^- and OH^- formation. Near-zero energy electrons are required for formation of HS^-. In all three cases, high pressures ($\sim 10^{-5}$ Torr) of precursor were necessary to produce reagent negative ion intensities adequate for study. Only drift-mode studies were performed in these cases.

Nitrites were prepared from CD_3OD and C_2H_5OH using standard methods.[25] Both PF_3 and OPF_3 were obtained from PCR and purified by trap-to-trap vacuum distillation. All other compounds used in these studies were obtained from commercial sources and used without further purification except for repeated freeze–pump–thaw cycles to remove noncondensable impurities.

Results

Negative Ions in OPF_3 and PF_3. In OFP_3 at low pressures (10^{-6} Torr) the negative ions O^- and F^- and a small amount of OPF_2^- have been observed in previous studies.[26] These ions are formed by dissociative electron attachment processes, with resonance maxima between 10 and 15 eV electron energy. Similarly, the ions F^-, F_2^-, PF^-, and PF_2^- have been produced in PF_3 at electron energies above 10 eV.[27] In both cases, cross sections for negative ion formation are small. With pressure, emission current, and electron energy conditions used in experiments described below, the negative ions noted above are not observed in samples of OPF_3 and PF_3.

In the case of OPF_3 at pressures above 10^{-5} Torr the negative ion $O_2PF_2^-$ (m/e 101) is observed with a resonance maxima for ion formation at 7.2 eV electron energy. No other ions are detected with increased pressure. This ion may result from a minor impurity. However, mass spectral analysis did not reveal the presence of other neutrals in the OPF_3 sample.[28]

In mixtures of OPF_3 and PF_3 with both H_2O and NH_3, ions are produced which show no double resonance from OH^- and NH_2^-. These ions (PF_2^- in PF_3 and OPF_2^- in OPF_3) are formed only in the presence of the second neutral. Double-resonance results eliminate the possibility of ion generation from ion–molecule reactions.[29] Surface reactions[28] or reactions on the electron filament[30] are possible. Neither of these ions is included in the figures presented.

Reactions of Nucleophiles with OPF_3. Figure 1 presents the variation of normalized ion intensity as a function of OPF_3 pressure in a mixture with 10^{-5} Torr NH_3. As NH_2^- (m/e 16) decreases, ions appear corresponding to $HNOPF_2^-$ (m/e 100) and $N(OPF_2)_2^-$ (m/e 185). As noted above OPF_2^- (m/e 85) is also detected in this mixture. Since it is not formed by reaction of NH_2^-, it is not included in Figure 1. Double-resonance experiments indicate that NH_2^- is the precursor to both product ions and further that $HNOPF_2^-$ reacts to form $N(OPF_2)_2^-$. There is no indication that $HNOPF_2^-$ and OPF_2^- are reactively coupled. Reactions 6 and 7 are consistent with these results.

$$NH_2^- + OPF_3 \rightarrow HNOPF_2^- + HF \quad (6)$$

$$HNOPF_2^- + OPF_3 \rightarrow N(OPF_2)_2^- + HF \quad (7)$$

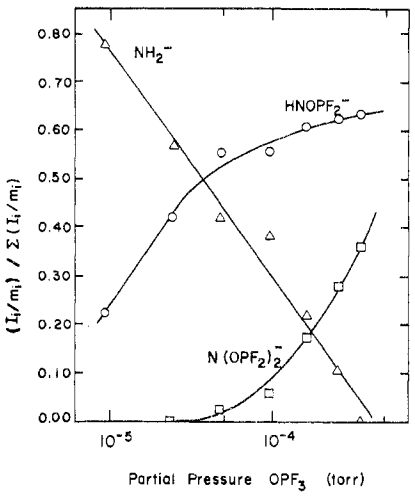

Figure 1. Variation of normalized negative ion intensity as a function of the partial pressure of OPF_3 in a mixture with 10^{-5} Torr NH_3 at 4.8 eV.

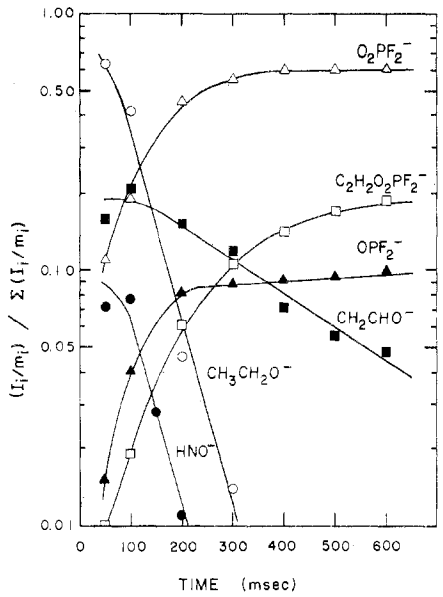

Figure 2. Temporal variation of normalized negative ion intensity in a mixture of CH_3CH_2ONO (1.00×10^{-7} Torr) and OPF_3 (1.76×10^{-6} Torr) at 20.0 eV.

Analogous nucleophilic reactions occur in mixtures of H_2O (eq 8) and H_2S (eq 9) with OPF_3. Although, as noted above,

$$OH^- + OPF_3 \rightarrow O_2PF_2^- + HF \quad (8)$$

$$SH^- + OPF_3 \rightarrow OSPF_2^- + HF \quad (9)$$

$O_2PF_2^-$ is formed in OPF_3 alone, double resonance indicates that $\sim$30% of the observed $O_2PF_2^-$ is formed by reaction with OH^-. Neither of the product ions reacts further with the neutrals present. Rates for reactions 6, 7, and 9, determined from single-resonance pressure studies, are presented in Table I. Because of complications due to other sources of $O_2PF_2^-$, a reaction rate for eq 8 could not be measured.

Figure 2 presents the temporal variation of ion intensity as a function of reaction time in a mixture of CH_3CH_2ONO (1×10^{-7} Torr) and OPF_3 (1.76×10^{-6} Torr). Product ions OPF_2^- (m/e 85), $O_2PF_2^-$ (m/e 101), and $C_2H_2O_2PF_2^-$ (m/e 127)[31] appear as a function of time. Double-resonance experiments confirm that $CH_3CH_2O^-$ reacts to produce $O_2PF_2^-$ (eq 10). At the low pressures of the trapped ion experiments and 20 eV electron energy, no $O_2PF_2^-$ is generated in OPF_3 alone. The complete disappearance of OPF_2^- and $C_2H_2O_2PF_2^-$ on double-resonance irradiation of HNO^- and CH_2CHO^-,

Table I. Summary of Gas-Phase Nucleophilic Reactions of OPF_3 and PF_3

Reacn	Eq no.	k_{exptl}[a]	k_{ADO}[b]	k_{exptl}[c]/k_{ADO}
$NH_2^- + OPF_3 \rightarrow NHOPF_2^- + HF$	6	16.5	20.6	0.80
$NHOPF_2^- + OPF_3 \rightarrow N(POF_2)_2^- + HF$	7	2.0	10.8	0.19
$OH^- + OPF_3 \rightarrow O_2PF_2^- + HF$	8		20.0	
$CH_3CH_2O^- + OPF_3 \rightarrow O_2PF_2^- + CH_3CH_2F$	10	11.6	13.7	0.85
$HNO^- + OPF_3 \rightarrow OPF_2^- + HF + NO$	11	11.9	15.7	0.76
$CH_2CHO^- + OPF_3 \rightarrow C_2H_2O_2PF_2^- + HF$	12	5.0	13.9	0.36
$SH^- + OPF_3 \rightarrow OSPF_2^- + HF$	9	1.2	15.4	0.08
$NH_2^- + PF_3 \rightarrow NHPF_2^- + HF$	13	7.9	15.1	0.96
$NH_2^- + PF_3 \rightarrow NPF^- + 2HF$	14	6.6		
$OH^- + PF_3 \rightarrow OPF_2^- + HF$	15		14.8	
$CH_3CH_2O^- + PF_3 \rightarrow OPF_2^- + CH_3CH_2F$	17	5.6	9.2	0.61
$HNO^- + PF_3 \rightarrow NOPF_2^- + HF$	18	5.0	11.8	0.42
$PF_2^- + H_2O \rightarrow OPF_2^- + H_2$	16		18.0	

[a] Experimental rate is determined as noted in text; in units of 10^{-10} cm^3 mol^{-1} s^{-1}. [b] Rate, in units of 10^{-10} cm^3 mol^{-1} s^{-1}, is calculated using the average dipole orientation model equation $k_{ADO} = [2\pi e/\mu^{1/2}][\alpha^{1/2} + c\mu_d(2/\pi kT)^{1/2}]$ in which μ is the reduced mass of the ion–molecule collision pair, α is the polarizability of the neutral, μ_d is the dipole moment of the neutral, and c is the constant estimated as noted in ref 36. Polarizabilities for OPF_3 and PF_3 are taken as 33.0×10^{-25} and 29.0×10^{-25} cm^3, respectively; see ref 41. Dipole moments for OPF_3 and PF_3 are taken as 1.74 and 1.03 D, respectively, from R. R. C. Carlson and D. W. Meek, *Inorg. Chem.*, **13**, 1741 (1974). [c] In those cases where two reaction pathways occur, the total rate is compared to the ADO rate.

respectively, indicate reactions 11 and 12. Rates for reactions 10–12 as determined from trapping studies are listed in Table I.

$$CH_3CH_2O^- + OPF_3 \rightarrow O_2PF_2^- + CH_3CH_2F \quad (10)$$

$$HNO^- + OPF_3 \rightarrow OPF_2^- + HF + NO \quad (11)$$

$$CH_2CHO^- + OPF_3 \rightarrow C_2H_2O_2PF_2^- + HF \quad (12)$$

Reactions of Nucleophiles with PF_3. On addition of PF_3 to 1×10^{-5} Torr NH_3 at 4.8 eV electron energy, ions detected are NH_2^- (*m/e* 16), NPF^- (*m/e* 64), PF_2^- (*m/e* 69), and $HNPF_2^-$ (*m/e* 84). As noted above, PF_2^- is not formed by reaction of NH_2^-. Double-resonance experiments confirm that NH_2^- reacts to form both $HNPF_2^-$ and NPF^- as in eq 13 and 14. No further reactions of these species are observed with the neutrals present.

$$NH_2^- + PF_3 \rightarrow HNPF_2^- + HF \quad (13)$$

$$NH_2^- + PF_3 \rightarrow NPF^- + 2HF \quad (14)$$

Ions PF_2^- (*m/e* 69) and OPF_2^- (*m/e* 85) appear as PF_3 is added to a sample of H_2O (2×10^{-5} Torr). Only the latter ion OPF_2^- is formed by reaction of PF_3 with OH^- (eq 15). Double resonance also indicates that PF_2^- reacts to form OPF_2^- (eq 16).

$$OH^- + PF_3 \rightarrow OPF_2^- + HF \quad (15)$$

$$PF_2^- + H_2O \rightarrow OPF_2^- + H_2 \quad (16)$$

The temporal variation of ion intensity in a mixture of CH_3CH_2ONO (1.20×10^{-7} Torr) and PF_3 (2.44×10^{-7} Torr) is presented in Figure 3. Product ions OPF_2^- (*m/e* 85) and $ONPF_2^-$ (*m/e* 99) appear at longer times. Reactions 17 and 18 are consistent with double-resonance experiments,

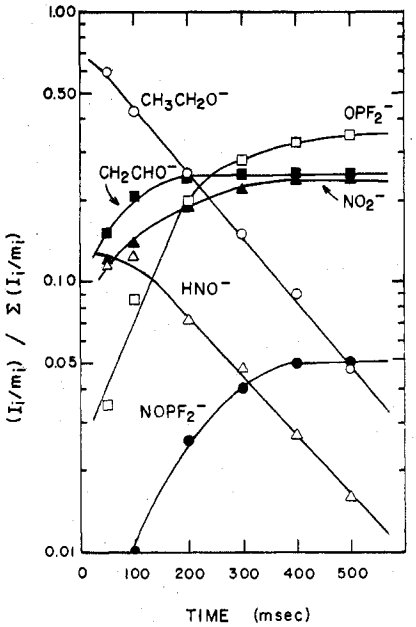

Figure 3. Temporal variation of normalized negative ion intensity in a mixture of CH_3CH_2ONO (1.20×10^{-7} Torr) and PF_3 (2.44×10^{-7} Torr) at 20.0 eV.

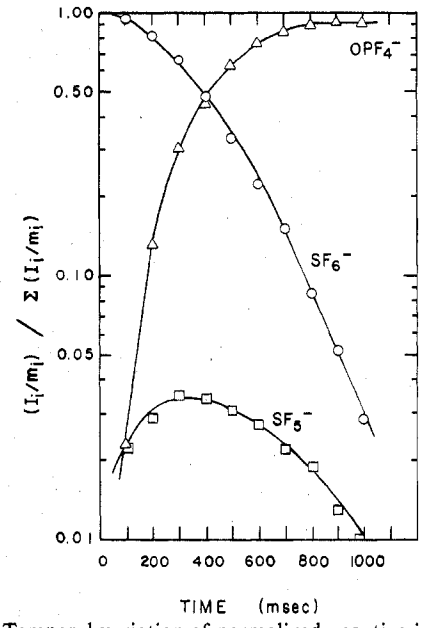

Figure 4. Temporal variation of normalized negative ion intensity in a mixture of OPF_3 (3.50×10^{-7} Torr) with a trace of SF_6 at 20.0 eV.

$$CH_3CH_2O^- + PF_3 \rightarrow OPF_2^- + CH_3CH_2F \quad (17)$$

$$HNO^- + PF_3 \rightarrow ONPF_2^- + HF \quad (18)$$

$CH_3CH_2O^-$ and HNO^- being the sole precursors of OPF_2^- and $NOPF_2^-$, respectively. The ion CH_2CHO^- (*m/e* 43) is unreactive in this mixture. Rates for reactions 13–18 are listed in Table I.

Fluoride-Transfer Reactions and Lewis Acidity of OPF_3. Figure 4 presents the temporal variation of normalized ion intensity in a mixture of 3.50×10^{-7} Torr OPF_3 with a trace amount ($<10^{-7}$ Torr) of SF_6. Both primary ions SF_6^- (*m/e* 146) and SF_5^- (*m/e* 127) decrease as a product ion OPF_4^- (*m/e* 123) appears. Double-resonance experiments link

Table II. Fluoride Bond Strengths[a]

M	D(M-F$^-$)[b]	M	D(M-F$^-$)[b]
PF_5	>71[c]	SF_4	54 ± 12[e]
BF_3	71[c]	$(CH_3)_3SiF$	50 ± 10
SiF_4	68.0	PF_3	50 ± 5[d]
$(CH_3)_2BF$	61.8	HCN	47 ± 3[f]
OPF_3	58.9[d]	SO_2	<45[f]
$(CH_3)_3B$	58.5	F	29 ± 3.0[g]
$(CH_3)_2SiF_2$	55.5	SF_5	11 ± 8[e]

[a] All values in kcal/mol at 298 K. [b] Binding energies of F$^-$ to boron and silicon compounds are taken from ref 32 and 15, respectively. [c] J. C. Haartz and D. H. McDaniel, *J. Am. Chem. Soc.*, **95**, 3562 (1973). [d] Present study. [e] Reference 19. [f] Reference 35. [g] Calculated using EA(F_2) = 3.09 ± 0.1 eV from W. A. Chupka, J. Berkowitz, and D. Gutman, *J. Chem. Phys.*, **55**, 2724 (1971).

production of OPF_4^- directly to SF_6^- (eq 19). A slower F$^-$ transfer from SF_5^- also occurs (eq 20).

$$SF_6^- + OPF_3 \rightarrow OPF_4^- + SF_5 \quad (19)$$

$$SF_5^- + OPF_3 \rightarrow OPF_4^- + SF_4 \quad (20)$$

Temporal variation of normalized ion intensity in a (1:1.9) mixture of OPF_3 and $(CH_3)_3B$ is presented in Figure 5. Ions $(CH_3)_3BF^-$ (m/e 75), $(CH_3)_2BF_2^-$ (m/e 79), OPF_4^- (m/e 123), and SF_5^- (m/e 127) appear and increase as SF_6^- (m/e 146) decays with time. Reactions 21–23, in addition to reactions 16 and 17, are consistent with observed double resonance. Reactions 21–23 have been investigated previously.[32] At long times equilibrium fluoride transfer occurs between OPF_4^- and $(CH_3)_3BF^-$ (eq 24). The equilibrium constant

$$SF_6^- + (CH_3)_3B \rightarrow \begin{cases} (CH_3)_2BF_2^- + SF_4 + CH_3 & (21) \\ SF_5^- + (CH_3)_2B + CH_3F & (22) \end{cases}$$

$$SF_5^- + (CH_3)_3B \rightarrow (CH_3)_3BF^- + SF_5 \quad (23)$$

$$(CH_3)_3BF^- + OPF_3 \rightleftharpoons OPF_4^- + (CH_3)_3B \quad (24)$$

(K_{eq}) for reaction 21 as written is determined to be 1.9 ± 0.4. Ion ejection techniques,[33] which allow measurement of the forward and reverse rate constants of reaction 24 (Table I), confirm this value for K_{eq}. Entropy contributions will be negligible,[34] so that $\Delta H \approx \Delta G$ and $D(OPF_3\text{–}F^-) - D[(CH_3)_3B\text{–}F^-] = 0.38 \pm 0.14$ kcal/mol. Using the estimated value $D[(CH_3)_3B\text{–}F^-] = 58.5 \pm 0.4$ kcal/mol (Table II), $D(OPF_3\text{–}F^-)$ is calculated as 58.9 ± 0.4 kcal/mol.

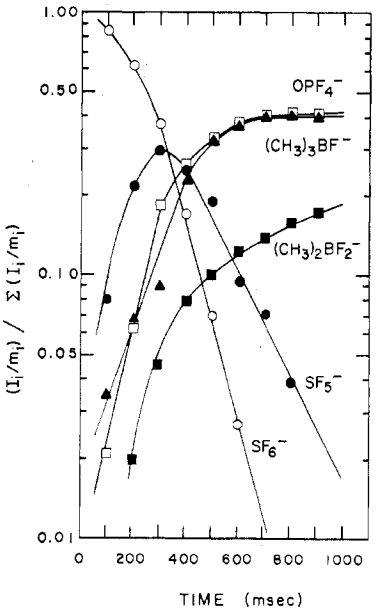

Figure 5. Temporal variation of normalized ion intensity in a mixture of OPF_3 (2.3×10^{-7} Torr) and $(CH_3)_3B$ (4.3×10^{-7} Torr) with a trace of SF_6 at 20.0 eV.

In the mixture of $(CH_3)_3B$ and OPF_3, fluoride transfer does not occur from $(CH_3)_2BF_2^-$ to OPF_3 (Figure 5). Further, $(CH_3)_2SiF_3^-$ produced in a mixture of $(CH_3)_2SiF_2$ and SF_6 by reaction 25 reacts with OPF_3 to form OPF_4^- (eq 26).

$$SF_5^- + (CH_3)_2SiF_2 \rightarrow (CH_3)_2SiF_3^- + SF_4 \quad (25)$$

$$(CH_3)_2SiF_3^- + OPF_3 \rightarrow OPF_4^- + (CH_3)_2SiF_2 \quad (26)$$

These results indicate limits for the bond strength in OPF_4^-, $61.8 > D(OPF_3\text{–}F^-) > 55.5$ kcal/mol, consistent with the measured bond strength noted above. Rates for F$^-$-transfer reactions to OPF_3 are summarized in Table III.

Fluoride-Transfer Reactions and Lewis Acidity of PF_3. In Figure 6, the temporal variation of ion intensity in a mixture of 7.2×10^{-7} Torr PF_3 with a trace of SF_6 is presented. As a function of reaction time, SF_6^- (m/e 146) decays as SF_5^- (m/e 127) and PF_4^- (m/e 107) appear. Reactions 27 and 28

$$SF_6^- + PF_3 \xrightarrow{0.94} SF_5^- + PF_4 \quad (27)$$

$$SF_6^- + PF_3 \xrightarrow{0.06} PF_4^- + SF_5 \quad (28)$$

Table III. Summary of Fluoride-Transfer Reactions

Reacn	Eq no.	k_{exptl}[a]	k_{ADO}[b]	k_{exptl}/k_{ADO}[c]	Thermochemical inference
$SF_6^- + OPF_3 \rightarrow OPF_4^- + SF_5$	19	3.1	9.8	0.32	$D(SF_5\text{–}F^-) < D(OPF_3\text{–}F^-)$
$SF_5^- + OPF_3 \rightarrow OPF_4^- + SF_4$	20	2.1	10.4	0.20	$D(SF_4\text{–}F^-) < D(OPF_3\text{–}F^-)$
$SF_6^- + (CH_3)_3B \rightarrow (CH_3)_2BF_2^- + SF_4 + CH_3$	21	1.4			
$SF_6^- + (CH_3)_3B \rightarrow SF_5^- + (CH_3)_2B + CH_3F$	22	3.7	10.4	0.49	
$SF_5^- + (CH_3)_3B \rightarrow (CH_3)_3BF^- + SF_4$	23	2.8	10.6	0.26	
$(CH_3)_3BF^- + OPF_3 \rightarrow OPF_4^- + (CH_3)_3B$	24[d]	3.1	11.7	0.26	$D(OPF_3\text{–}F^-) = 58.9 \pm 0.4$ kcal/mol
$OPF_4^- + (CH_3)_3B \rightarrow (CH_3)_3BF^- + OPF_3$	24[e]	1.7	10.7	0.16	
$(CH_3)_2SiF_3^- + OPF_3 \rightarrow OPF_4^- + (CH_3)_2SiF_2$	26	2.87	10.4	0.27	$D[(CH_3)_2SiF_2\text{–}F^-) < D(OPF_3\text{–}F^-)$
$SF_6^- + PF_3 \rightarrow SF_5^- + PF_4$	27	0.95			
$SF_6^- + PF_3 \rightarrow PF_4^- + SF_5$	28	0.04	7.7	0.13	$D(SF_5\text{–}F^-) < D(PF_3\text{–}F^-)$
$F_2^- + PF_3 \rightarrow PF_4^- + F$	30	*f*			$D(F\text{–}F^-) < D(PF_3\text{–}F^-)$
$SO_2F^- + PF_3 \rightarrow PF_4^- + SO_2$	31	*f*			$D(SO_2\text{–}F^-) < D(PF_3\text{–}F^-)$
$PF_4^- + OPF_3 \rightarrow OPF_4^- + PF_3$	32	*f*			$D(PF_3\text{–}F^-) < D(OPF_3\text{–}F^-)$
$(CH_3)_3SiF_2^- + PF_4^- + (CH_3)_3SiF$	33	*f*			$D[(CH_3)_3SiF\text{–}F^-] < D(PF_3\text{–}F^-)$
$FHCN^- + PF_3 \rightarrow PF_4^- + HCN$	34	*f*			$D(CNH\text{–}F^-) < D(PF_3\text{–}F^-)$

[a] Experimental rate is determined as noted in the text; in units of 10^{-10} cm^3 mol^{-1} s^{-1}. [b] In units 10^{-10} cm^3 mol^{-1} s^{-1}; calculated as noted in Table I. The Langevain rate equation is used for nonpolar molecules [$k_L = 2\pi e(\alpha/\mu)^{1/2}$]; $\alpha[(CH_3)_3B]$ was taken from ref 32. [c] In those cases in which two reaction pathways occur, the total rate is compared to the calculated rate. [d] Reaction 24, forward direction. [e] Reaction 24, reverse direction. [f] Reaction observed at thermal ion energies but rate not measured.

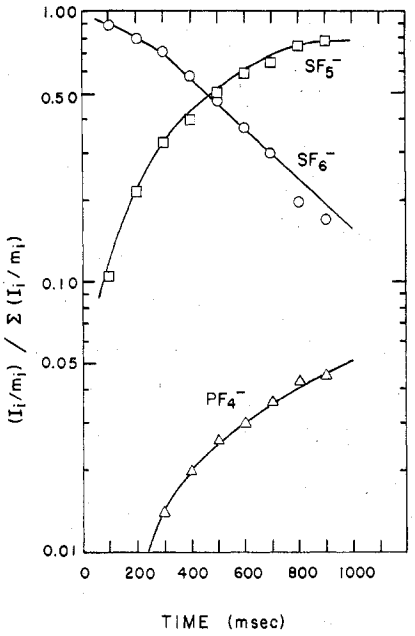

Figure 6. Temporal variation of normalized ion intensity in a mixture of PF_3 (9.74×10^{-7} Torr) with a trace of SF_6 at 20.0 eV.

are confirmed by double-resonance experiments. The fluoride-transfer reaction 29 does not occur at thermal ion

$$SF_5^- + PF_3 \rightarrow PF_4^- + SF_4 \quad (29)$$

energies but is effected by irradiating SF_5^- in double-resonance experiments, suggesting that this process is endothermic. In mixtures of OPF_3, PF_3, and a trace of SF_6, no PF_4^- is observed, due to the competing and much faster process 19.

Negative ions F^- (*m/e* 19, 60%), F_2^- (*m/e* 38, 11%), and SO_2F^- (*m/e* 85, 29%) are generated by electron impact in moderate pressures (5×10^{-6} Torr) of SO_2F_2.[19] In a mixture of PF_3 with SO_2F_2, PF_4^- (*m/e* 107) is produced by F^- transfer from F_2^- (eq 30) and SO_2F^- (eq 31).

$$F_2^- + PF_3 \rightarrow PF_4^- + F \quad (30)$$

$$SO_2F^- + PF_3 \rightarrow PF_4^- + SO_2 \quad (31)$$

On addition of OPF_3 and PF_3 to SO_2F_2, OPF_4^- and PF_4^- can be observed. Double resonance confirms that F^- transfer occurs only from PF_4^- to OPF_3 (eq 32). In similar experi-

$$PF_4^- + OPF_3 \rightarrow OPF_4^- + PF_3 \quad (32)$$

ments using mixtures of SO_2F_2 with $(CH_3)_3SiF$ and HCN, F^--transfer processes generate $(CH_3)_3SiF_2^-$ (*m/e* 111) and $FHCN^-$ (*m/e* 46), respectively. Both of these ions transfer F^- to PF_3 (eq 33 and 34). An ordering of F^- bond strengths

$$(CH_3)_3SiF_2^- + PF_3 \rightarrow PF_4^- + (CH_3)_3SiF \quad (33)$$

$$FHCN^- + PF_3 \rightarrow PF_4^- + HCN \quad (34)$$

$D(SO_2\text{–}F^-) < D(NCH\text{–}F^-) < D(PF_3\text{–}F^-) < D(SF_4\text{–}F^-)$ is consistent with these results. Although $D(SO_2\text{–}F^-)$ and $D(NCH\text{–}F^-)$ are not well-known, estimates[35] lead to limits of $45 < D(PF_3\text{–}F^-) < 54$ kcal/mol. Fluoride-transfer reactions are summarized in Table II.

Discussion

Nucleophilic Reactivity. In Table I, rate constants for reactions of OPF_3 and PF_3 with gas-phase bases are summarized. Experimental rates are compared to collision rates, calculated using the average dipole orientation (ADO) model[36] to account for the dipole moment of the neutral reactants. There is a general trend of increased rate with measured base strength. The low nucleophilic reactivity of HS^- (compared to NH_2^- and OH^-) has analogies in gas-phase studies of nucleophilic attack at carbon.[12b]

Scheme I

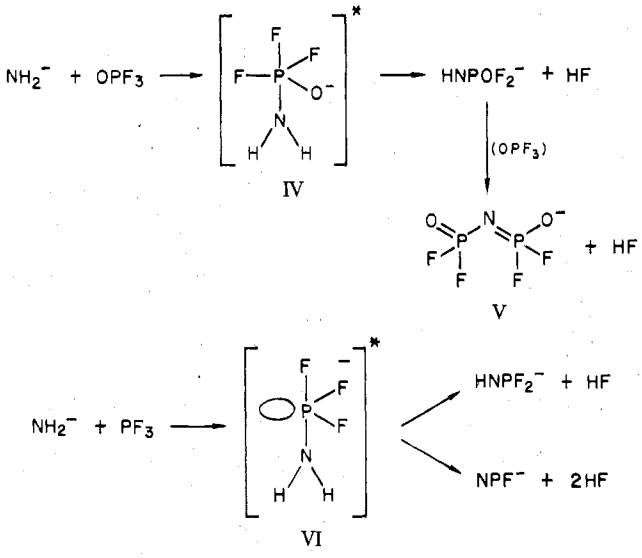

IV V VI

Scheme II

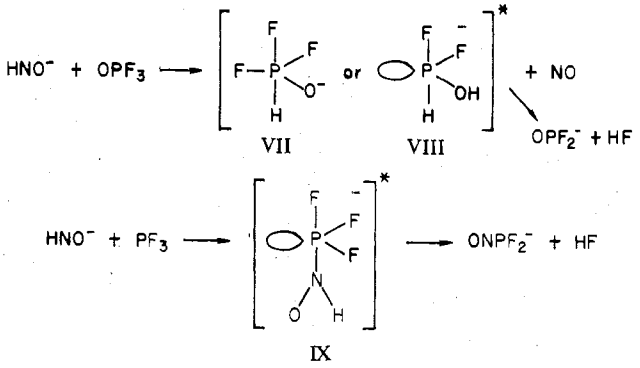

VII VIII IX

The reactions of OPF_3 and PF_3 with anionic bases can be described as the result of the decomposition of penta- and tetracoordinate intermediates. In the reaction of NH_2^- with OPF_3 (Scheme I) a pentacoordinate intermediate IV is proposed which dissociates by elimination of HF. The initial product $HNOPF_2^-$ reacts further with OPF_3 to form $N(OPF_2)_2^-$, presumably a nitrogen-bridged anion (V). In contrast, the reaction of NH_2^- with PF_3 results in two products $HNPF_2^-$ and NPF^- (Scheme I). The intermediate in this case, VI, also dissociates by elimination of HF. The product $HNPF_2^-$ may be formed with sufficient internal excitation for further decomposition to occur, leading to NPF^-. While the proposed intermediates in Scheme I are helpful in visualizing the reaction processes, there is no experimental evidence to justify their representation as shown. Criteria for structuring five-coordinate intermediates are discussed elsewhere.[2c]

In the present study, $O_2PF_2^-$, $OSPF_2^-$, and OPF_2^- do not react further with the neutrals examined. In solution these ions are weakly nucleophilic, displacing halides from phosphoryl and carbonyl compounds.[1] Direct displacement of F^- in gas-phase ion–molecule reactions is often very slow ($k \approx 10^{-12}$ cm^3 mol^{-1} s^{-1}) and is not observed when these anions interact with OPF_3 or PF_3.[37] Futhermore, since these species do not possess H or alkyl groups to form an energetically favorable neutral leaving group (HF or RF), they are unreactive in these systems.

There are several interesting mechanistic possibilities for the reactions of HNO^- and OPF_3 and PF_3 (Scheme II). In reactions with alkyl boranes, for example with $(CH_3)_3B$ (eq 35), HNO^- acts as a hydride donor. With stronger acids such as HCO_2H, an apparent proton transfer occurs[38] (eq 36) with

$$HNO^- + (CH_3)_3B \rightarrow (CH_3)_3BH^- + NO \quad (35)$$

$$HNO^- + HCO_2H \rightarrow HCO_2^- + H_2 + NO \quad (36)$$

H_2 and NO assumed to be the neutral products. Reaction 36 could proceed as a proton transfer or by decomposition of a chemically activated hydride-transfer product $[H_2CO_2H^-]^*$. In reaction of OPF_3 and HNO^-, proton transfer is impossible. The formation of an energetic hydride-transfer intermediate such as VII and VIII in Scheme II is feasible, however. The intermediate VIII may also be formed in reaction 15 of OH^- with PF_3. Either of these intermediates could decompose by elimination of HF. The formation of $ONPF_2^-$ by reaction of HNO^- with PF_3 suggests a more complicated process. Direct complexation of HNO^- to PF_3 as in intermediate IX in Scheme II, followed by elimination of HF, is a possible pathway to the observed ionic product. Since the adducts VII–IX are not directly observed, there is no experimental evidence for their existence.

Fluoride-Transfer Reactions and Lewis Acidities. Relative Lewis acidities are determined by measurement of the dissociation energies of acid–base complexes, such as R_3B–NR_3. A wide range of such complexes are formed with PF_5 acting as an acid. Trivalent phosphorus(III) compounds are generally considered as electron donors, but weakly bound complexes of PF_3 with tertiary amines have been reported.[39] Previously, OPF_3 has been observed to behave only as a base, with bonding through oxygen.[40] A comparison of the relative abilities of OPF_3, PF_3, and PF_5 to bind F^- is seen in their reaction with CsF in solution.[41] With PF_5, the salt $Cs^+PF_6^-$ is readily produced on treatment of PF_5 with CsF. The species $Cs^+OPF_4^-$ and $Cs^+PF_4^-$ have not been observed under similar conditions with OFP_3 and PF_3. In these cases, more complicated reactions occur to form the more stable $Cs^+PF_6^-$ (eq 37) and $Cs^+O_2PF_2^-$ (eq 38). These solution results indicate

$$5PF_3 + 3CsF \rightarrow 3Cs^+PF_6^- + 2P \quad (37)$$

$$2OPF_3 + 2CsF \rightarrow Cs^+O_2PF_2^- + Cs^+PF_6^- \quad (38)$$

that Lewis acidity should decrease in the order $PF_5 \gg PF_3 > OPF_3$.

Gas-phase Lewis acidities toward F^-, as measured using ICR techniques, decrease in the somewhat different order $PF_5 > OPF_3 > PF_3$ (Table III).[42] The susceptibility of OPF_3 to nucleophilic attack is strong evidence that OPF_3 acts as an electron acceptor, consistent with the present results. Kinetic instability rather than thermodynamic instability may prevent the observation of base complexes with OPF_3 in solution. Alternatively, differential solvation effects may cause the inversion of acidities in solution.

The relative acidities of PF_5, OPF_3, and PF_3 toward F^- as a reference base reflect the decreasing electron density at phosphorus. The ordering observed in this study parallels the increase in Lewis acidities of fluorinated methylsilanes with increased number of fluorine ligands: $(CH_3)_3SiF < (CH_3)_2SiF_2 < CH_3SiF_3$[15] (Table II). The failure to observe F^- adduct formation with alkyl phosphate esters and the predominance of nucleophilic attack at carbon in these compounds is then consistent with the lower electronegativity of alkoxide groups compared to that of fluorine. These results suggest that fluorinated phosphate esters (i.e., $OPF(OCH_3)_2$) may have moderate gas-phase Lewis acidities toward F^- as a base. If this is true, anionic fluorine transfer will be a useful method for chemical ionization detection[16] of these compounds.[43]

In conclusion, anionic nucleophilic attack on OPF_3 and PF_3 occurs at phosphorus with anionic products being the result of HF elimination from tetra- and pentacoordinated intermediates. Reaction is enhanced with increased basicity of the attacking anion. This is in contrast to the reactivity of alkyl phosphate esters, in which anionic attack occurs preferentially at carbon. Fluoride-transfer reactions suggest that OPF_3 and PF_3 are considerably stronger Lewis acids than phosphorus esters. Both of these differences appear to be a consequence of the decreased electron density at phosphorus in OPF_3 and PF_3 which is imposed by the electronegative fluorine ligands.

Finally, reaction 27 deserves special comment. The bond dissociation energy $D(SF_5^-\text{–F})$ is low, 11 kcal/mol (Table II). The bond dissociation energy $D(PF_4\text{–F})$ is probably substantially higher (the average of the first two P–F bond energies in PF_5 is 90 kcal/mol), making reaction 27 quite exothermic. Since SF_5^- does not react with PF_3, this mixture of gases can be utilized to generate the reagent ion SF_5^- for use in negative ion chemical ionization experiments. This avoids some of the more complex processes (e.g., reaction 21) which occur when SF_6^- is present in abundance.

Acknowledgment. This research was supported in part by the U.S. Army Research Office under Grant No. DAAG29-76-G-0274.

Registry No. PF_3, 7783-55-3; OPF_3, 13478-20-1; NH_2^-, 17655-31-1; OH^-, 14280-30-9; $CH_3CH_2O^-$, 16331-64-9; HNO^-, 66057-02-1; HS^-, 15035-72-0; SF_6^-, 25031-39-4; SF_5^-, 31140-82-6; CH_2CHO^-, 35731-40-9.

References and Notes

(1) A. J. Kirby and S. G. Warren, "The Organic Chemistry of Phosphorus", Elsevier, Amsterdam, 1967.
(2) (a) G. M. Kosolapoff and L. Maier, "Organic Phosphorus Compounds", Wiley-Interscience, New York, N.Y., 1972; (b) J. R. Van Wazer, "Phosphorus and Its Compounds", Interscience, New York, N.Y., 1956; (c) R. F. Hudson and C. Brown, *Acc. Chem. Res.*, **5**, 204 (1971).
(3) Attack and displacement at phosphoryl groups is important in biological energy-transfer processes; see ref 2b.
(4) D. B. Denny, A. K Tsolis, and K. Mislow, *J. Am. Chem. Soc.*, **84**, 4486 (1964).
(5) I. Dostrovsky and M. Halmann, *J. Chem. Soc.*, 1004 (1956).
(6) D. Samuel and B. L. Silver, *Adv. Phys. Org. Chem.*, **3**, 123 (1965).
(7) K. W. Hausen and L. S. Bartell, *Inorg. Chem.*, **4**, 1775 (1965).
(8) E. R. Kyba, *J. Am. Chem. Soc.*, **97**, 2554 (1975); **98**, 4805 (1976).
(9) S. A. Sullivan and J. L. Beauchamp, *J. Am. Chem. Soc.*, **99**, 5017 (1977).
(10) J. F. G. Faigle, P. C. Isolani, and S. M. Riveros, *J. Am. Chem. Soc.*, **98**, 2049 (1976).
(11) J. A. Bowie and B. D. Williams, *Aust. J. Chem.*, **27**, 1923 (1974).
(12) (a) O. I. Asubiojo, L. K. Blair, and J. I. Brauman, *J. Am. Chem. Soc.*, **97**, 6685 (1975); (b) W. N. Olmstead and J. I. Brauman, *ibid.*, **99**, 4219 (1977).
(13) R. V. Hodges, S. A. Sullivan, and J. L. Beauchamp, unpublished results.
(14) N. T. Thuong, *Bull. Soc. Chim. Fr.*, 928 (1971).
(15) M. K. Murphy and J. L. Beauchamp, *J. Am. Chem. Soc.*, **99**, 4992 (1977).
(16) See, for example, H. P. Tannenbaum, J. D. Roberts, and R. C. Dougherty, *Anal. Chem.*, **47**, 49 (1975).
(17) J. L. Beauchamp, *Annu. Rev. Phys. Chem.*, **22**, 527 (1972).
(18) T. B. McMahon and J. L. Beauchamp, *Rev. Sci. Instrum.*, **43**, 509 (1972).
(19) M. S. Foster and J. L. Beauchamp, unpublished results.
(20) A. G. Marshall and S. E. Buttrill, Jr., *J. Chem. Phys.*, **52**, 2750 (1970); T. B. McMahon, Ph.D. Thesis, California Institute of Technology, Pasadena, Calif., 1973, Chapter V.
(21) R. W. Odom, D. L. Smith, and J. H. Futrell, *Chem. Phys. Lett.*, **24**, 227 (1974); M. S. Foster and J. L. Beauchamp, *ibid.*, **31**, 482 (1975).
(22) K. Jaeger and A. Heinglein, *Z. Naturforsch., A*, **222**, 700 (1967).
(23) J. G. Dillard, *Chem. Rev.*, **73**, 590 (1973).
(24) G. E. Melton and G. A. Neece, *J. Am. Chem. Soc.*, **93**, 6757 (1971).
(25) W. A. Noyes, *Org. Synth.*, **2**, 108 (1943).
(26) T. C. Rhyne and J. G. Dillard, *Int. J. Mass Spectrom. Ion Phys.*, **7**, 371 (1971).
(27) K. A. G. MacNeil and J. C. J. Thynne, *J. Phys. Chem.*, **74**, 2257 (1970).
(28) These ionic species may be formed by electron attachment to trace impurities or neutral products of surface reactions. Similar processes may generate Cl_2^- in CF_2CFCl: see S. A. Sullivan and J. L. Beauchamp, *Chem. Phys. Lett.*, **48**, 294 (1977).
(29) OH^- is generated by a very fast reaction of H^- with H_2O: $H^- + H_2O \rightarrow OH^- + HO$ (see ref 24). Similar processes (i.e., $H^- + PF_3 \rightarrow PF_2^- + HF$) are possible in these systems but could not be detected in double-resonance experiments.
(30) J. L. Beauchamp, *J. Chem. Phys.*, **64**, 929 (1976).
(31) The chemical formula of this ion is inferred from its mass and precursor. The ion structure has not been established.
(32) M. K. Murphy and J. L. Beauchamp, *J. Am. Chem. Soc.*, **98**, 1433 (1976); M. K. Murphy and J. L. Beauchamp, **16**, 2437 (1977).
(33) B. S. Freiser, T. B. McMahon, and J. L. Beauchamp, *Int. J. Mass Spectrom. Ion Phys.*, **12**, 249 (1973).
(34) Entropy effects in equilibrium reaction 21 are estimated to be negligible by comparison of ΔS_{298} of OPF_3, $(CH_3)_3B$, PF_5, and $(CH_3)_3CF$. The latter two species are isoelectronic with the reactant ions OPF_4^- and $(CH_3)_3BF^-$, respectively: see S. W. Benson, "Thermochemical Kinetics",

2nd ed., Wiley, New York, N.Y., 1976.
(35) S. A. Sullivan and J. L. Beauchamp, unpublished results.
(36) L. Bass, T. Su, W. J. Chesnavich, and M. T. Bowers, *Chem. Phys. Lett.*, **34**, 119 (1975).
(37) D. K. Bohme, G. J. Mackay, and J. D. Payzant, *J. Am. Chem. Soc.*, **96**, 4027 (1974).
(38) S. A. Sullivan, Ph.D. Thesis, California Institute of Technology, Pasadena, Calif., 1977.
(39) R. R. Holmes, W. P. Gallagher, and R. P. Carter, Jr., *Inorg. Chem.*, **2**, 437 (1963); E. L. Muetterties and W. Mahler, *ibid.*, **4**, 119 (1965).
(40) R. R. Holmes and J. A. Forstner, *Inorg. Chem.*, **2**, 380 (1963); R. R. Holmes, *J. Am. Chem. Soc.*, **82**, 5285 (1960).
(41) M. Lustig and J. K. Ruff, *Inorg. Chem.*, **6**, 2115 (1967).
(42) A previous gas-phase study suggests the relative F^- binding energies decrease $PF_5^- > PF_4^- > OPF_4^-$: T. C. Rhyne and J. G. Dillard, *J. Am. Chem. Soc.*, **91**, 6521 (1969); T. C. Rhyne and J. G. Dillard, *Inorg. Chem.*, **10**, 730 (1971). This ordering is based on relative cross sections for F^- transfer from SF_6^-. Rates do not necessarily reflect thermochemistry: see J. C. Haartz and D. H. McDaniel, *J. Am. Chem. Soc.*, **95**, 3562 (1973).
(43) Fluorophosphonates are used widely as pesticides. The high human toxicities of some of these compounds necessitate the development of sensitive and specific methods of detection: see R. D. O'Brien, "Toxic Phosphorus Esters: Chemistry, Metabolism and Biological Effects", Academic Press, New York, N.Y., 1960.

Contribution from the Department of Chemistry, University of Western Ontario, London, Ontario, Canada, N6A 5B7, and Institute of Physics, Uppsala University, S-751 21 Uppsala 1, Sweden

Gas-Phase ESCA Studies of Valence and Core Levels in XeF_2 and XeF_4

G. M. BANCROFT,*[1a] P.-Å. MALMQUIST,[1b] S. SVENSSON,[1b] E. BASILIER,[1b] U. GELIUS,[1b] and K. SIEGBAHN[1b]

Received January 17, 1978

Using monochromatized Al Kα radiation, we have made a detailed gas-phase ESCA study of the valence levels and Xe 3d and 4d core levels in XeF_2 and XeF_4. The valence band peaks have been assigned to the molecular orbitals previously calculated. Several previous experimental and theoretical assignments are shown to be incorrect. Agreement is generally good between our observed positions and intensities and the calculated values. The observed broadening of the compound Xe 3d and 4d peaks (relative to the corresponding Xe gas peaks) is shown to be due to the C_2^0 asymmetry term in the ligand field expansion. The broadening of the 4d levels of 0.12 ± 0.02 eV (XeF_2) and 0.19 ± 0.02 eV (XeF_4) leads to a $4d_{3/2}$ splitting of 0.33 ± 0.04 eV (XeF_2) and 0.40 ± 0.04 eV (XeF_4). These values are in excellent agreement with the $d_{3/2}$ splittings derived in previous absorption studies. The derived C_2^0 terms [+0.041 ± 0.004 eV (XeF_2) and −0.045 ± 0.004 eV (XeF_4)] are also in excellent agreement with those previously determined. The average 3d broadening of 0.06 ± 0.02 eV for the two compounds leads to a $3d_{3/2}$ splitting of 0.18 ± 0.06 eV and a $|C_2^0|$ value of 0.021 ± 0.006 eV. These are in good agreement with the normalized theoretical values. The anomalous electron spectrum in the 4s–4p range was found to change upon fluoridization. Similar effects are seen when the nuclear charge is changed and can be qualitatively explained in terms of the energy difference between doubly ionized states and the unperturbed 4p hole state.

Introduction

Several recent papers have reported gas-phase ESCA[2] and UV (He I and He II) photoelectron[3,4] spectra of the xenon fluorides. In addition, there has been considerable interest in the absorption spectra of these compounds.[5,6] An ab initio SCF MO calculation[7] has been useful for assigning parts of the valence band spectra[3,4] and for calculating the observed[5] ligand field splitting of the Xe 4d levels in XeF_2 and XeF_4.

However, a number of ambiguities still exist in the valence band assignments, and the valence levels above 18 eV binding energy have not been observed and/or unambiguously assigned. There is also confusion about the role of ligand field splitting on core levels in these and other spectra. Ligand field broadening and splitting,[8] due to the asymmetry crystal field term C_2^0, has been observed recently in the photoelectron spectra of Sn and Cd 4d levels.[9] A similar Xe 4d splitting was also reported in the absorption studies of XeF_2 and XeF_4.[5] However, Carroll et al.[2b] ruled out ligand field splitting of the Xe 3d lines as being unimportant in 3d line broadening. In contrast, Basch's calculations,[7] Gupta and Sen's calculations,[8] and previous experimental results on Sn compounds[10] indicated that the 3d ligand field splitting should approach half of the 4d ligand field splitting.

In addition to the above xenon fluoride results, there have been recent ESCA studies of the interesting 4p region of the xenon gas spectrum.[11,12] The apparent absence of the $4p_{1/2}$ peak is due to configuration interaction of $4d^8 5s^2 5p^6 nl$ states with the 4p single hole state. The nature of this 4p spectrum should change appreciably with the number of F ligands.

We have undertaken a high-resolution ESCA study of the 3d, 4d, and valence band levels of XeF_2 and XeF_4 with three objectives: to clear up the ambiguities in the assignment of the valence levels, to measure accurately the ligand field broadening of both the 3d and 4d Xe core levels, and to examine changes in the 4p structure. We also derive cross section ratios which are compared with current theoretical values and comment on differences in chemical shifts for the 3d and 4d orbitals.

Experimental Section

The gas-phase spectra of XeF_2 and XeF_4 were recorded using the electrostatic ESCA instrument,[13] which incorporates a fine-focusing monochromatized Al Kα x-ray source and multidetection system. The compounds were purchased from L'Air Liquid in France, and high-purity Xe gas was used as reference. To prevent extensive decomposition of the fluorides, all handling of the compounds was done in an Ar-filled drybag, and all inlet parts of the spectrometer were coated with Teflon spray. In this way, we were able to obtain spectra of the fluorides free of the decomposition products in a relatively short time. The intense 3d core levels were often monitored during the accumulation of the valence band spectra to ensure that no decomposition to Xe gas was occurring. For the Xe 3d and 4d line width studies, we ran spectra of xenon gas and the compound simultaneously. A number of high-quality spectra were accumulated for these core levels to provide good statistical data.

The spectra were computer fitted using standard iterative methods to Gaussian and/or Gauss–Lorentz combination functions. When Gauss–Lorentz functions were used for the core levels, statistically acceptable χ^2 values (the sum of the squares of the deviations from the best fit divided by the variances) were obtained. For example, for the XeF_2 (and Xe) 4d spectra, χ^2 values of ~150 (~130 degrees of freedom) were obtained.

Results and Discussion

Valence Band Spectra. The valence band region of the XeF_2 and XeF_4 electron spectra is illustrated in Figure 1. Assignments, binding energies, and intensity data are given in Table I. The theoretical binding enegies in Table I are 0.92 times the calculated orbital energies, a figure found

0020-1669/78/1317-1595$01.00/0 © 1978 American Chemical Society